

Evaluation of Kromoscopy: resolution of glucose and urea

Anna M. Helwig, Mark A. Arnold, and Gary W. Small

Kromoscopy involves the transmission of a broad band of electromagnetic radiation through the sample of interest. The transmitted light is collected and divided evenly into four detector channels with complementary bandpass functions. This optical configuration provides high signal-to-noise ratios that are ideal for analytical measurements. The molecular basis of the four-channel response is critical, because it directly influences selectivity of the measurement and, therefore, the feasibility of applications in complex sample matrices. Selectivity of the Kromoscopic signal is demonstrated by resolution of glucose and urea with four channels of information collected over the 800–1300-nm near-infrared spectral region. Analysis of the individual channel responses indicates that the displacement of water from the optical path by the dissolution of solute is a major component of the Kromoscopic measurement in this spectral region. Nevertheless, significant differences are observed in channel responses for glucose and urea. A three-dimensional vector plot of the data highlights these differences and reveals unique vector directions for glucose and urea. This difference in direction of the response vectors represents the principal basis for distinguishing glucose and urea dissolved in aqueous solutions.

© 2000 Optical Society of America

OCIS codes: 000.2170, 170.3890, 170.1610, 120.3890, 000.1570.

1. Introduction

Kromoscopy has been proposed as a method for measuring blood glucose noninvasively in human subjects.^{1–12} In Kromoscopy, white light passes through the sample of interest, and the resulting transmitted light is equally divided into four separate channels for detection. Each detector channel responds to a portion of the full spectral bandwidth of the incident radiation. An optical filter positioned immediately before the detector element defines the spectral response of each individual channel, and the filters are selected to provide overlapping response functions for the channels. The high throughput of this optical configuration provides large signal-to-noise ratios. Congruency of the measured optical signals further enhances signal to noise by providing a means for eliminating common-mode (i.e., correlated) noise between channels.

Near-infrared (NIR) absorption spectroscopy has also been suggested as a means for measuring glucose noninvasively in samples of biological origin.^{13–16} In this conventional approach, individual absorptions are measured at each wavelength across the spectral region of interest. Multivariate calibration methods, such as partial least-squares regression, are then used to correlate variations in the spectral data with known changes in analyte concentration. In the partial least squares algorithm, the dimensionality of the spectral data (dependent variable) is reduced by computation of a set of orthogonal factors to represent those portions of the spectral data that most strongly correlate with analyte concentration (independent variable). Similarly, the broadband channels of the Kromoscopy experiment effectively reduce the dimensionality of the analytical measurement across the entire spectrum of analysis. In the Kromoscopic analysis, however, signal-to-noise enhancements can be realized with a relatively simple and robust instrument configuration (i.e., no interferometer or dispersion element).

Early descriptions of both the technique and the capabilities of Kromoscopy pertain to measurements in the short-wavelength (sw) region of the NIR spectrum (0.7–1.4 μm).^{1–4} Absorption features for glucose in this spectral region are extremely weak and correspond to high-order overtones and combinations of CH and OH vibrations.^{17,18} Absorptivities of

A. M. Helwig and M. A. Arnold (mark-arnold@uiowa.edu) are with the Department of Chemistry and Optical Science and Technology Center, University of Iowa, Iowa City, Iowa 52242. G. W. Small is with the Department of Chemistry and Center for Intelligent Chemical Instrumentation, Ohio University, Athens, Ohio 45701.

Received 6 December 1999; revised manuscript received 6 June 2000.

0003-6935/00/254715-06\$15.00/0

© 2000 Optical Society of America

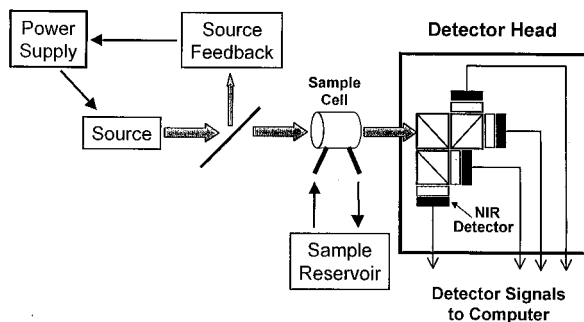


Fig. 1. Schematic diagram of the four-channel instrument used to collect the Kromoscopic responses.

these transitions are so weak that absorbance spectra of glucose in aqueous solutions are dominated by the absorption features of water. Indeed, absorbance spectra of aqueous glucose solutions display negative absorption features, which correspond to the displacement of water by the dissolved glucose molecules.

The objective of our initial evaluation of Kromoscopy is to establish the origin of information present in the Kromoscopic signal. Before Kromoscopy can be considered a practical method for measuring glucose noninvasively in complex biological matrices, like the human body, it must be established that the information originates from molecular glucose. It is not acceptable for the information to originate from a secondary effect created by the glucose molecule, such as water displacement.

Here we detail a comparison of Kromoscopic responses for glucose and urea. Results indicate that water displacement is a major component in the Kromoscopic response for each of these analytes. Nevertheless, a secondary component of these responses reveals reproducible and significant differences between responses for glucose and urea. The uniqueness of the glucose and urea responses supports the contention that analyte-specific information is available in the four-channel signals of the Kromoscopy experiment.

2. Apparatus

The experimental apparatus used to collect the Kromoscopic data is presented schematically in Fig. 1. Incident radiation was supplied by a 20-W tungsten-halogen lamp. Power for the lamp was provided by an Oriel Model 68831 power supply, and the lamp power was regulated by an Oriel Model 68850 feedback controller. Light collected from the source was collimated, and a fraction of the collimated beam (ca. 10%) was directed by a beam splitter to this feedback controller. The remaining incident beam was transmitted through a 2-cm flow through sample cell constructed from Infrasil quartz (Model 34-I-20, Starna Cells, Atascadero, California). The incident light was restricted by a 13-mm aperture positioned immediately before the cell.

A four-channel detector module was used for mea-

suring the transmitted radiation. In this module, the transmitted light passes through a set of three beam splitters designed to divide the entering radiation into four equivalent detector channels. Radiant powers were measured simultaneously at each channel by use of individual, room-temperature germanium photodiode detectors (EG&G Judson, Montgomeryville, Pennsylvania). A unique band-pass filter was positioned before each detector to define the spectral response for that channel. Signals from each detector channel were amplified, converted to digital signals, and recorded by a computer. Analog-to-digital conversion was performed by four separate Hewlett Packard Model 3458A multimeters. Signals from the four multimeters were collected by a single computer (HP Vectra VA) by use of IEEE-488.2 PCI-GRIB interface boards (National Instruments, Austin, Texas) coupled with Labview software (version 4.01). The analog-to-digital conversion was performed at 50 Hz and was controlled by a 50-Hz square-wave signal taken from a common function generator (BK Precision, Model 4011). This instrumental configuration provided a signal-to-noise ratio of approximately 40,000 for each channel.

3. Experimental Methods

Glucose and urea were used as received from Aldrich Chemical Co. (Milwaukee, Wisconsin). All solutions were prepared with distilled-deionized water that was obtained by passing house-distilled water through a three-stage Milli-Q water purification unit (Millipore Corp., Bedford, Massachusetts).

Channel intensities were measured as the temperature-controlled solution passed through the flow through sample cell. To initiate an experiment, we placed 3.0 l of buffer (0.05-M phosphate buffer at pH 6.86) in the clean, dry solution reservoir of a temperature bath (Model 90, Fisher Scientific, Itasca, Illinois). Two segments of thick-walled Tygon tubing were used to connect the output of the water bath to the input of the sample cell and then from the sample cell back to the water bath. Solution within the bath circulated continuously through the sample cell, and the temperature of the circulating solution was controlled at 39.8 °C. A thermocouple probe was positioned in the flow stream immediately before the sample cell for monitoring the solution temperature. A nylon gas-liquid filter was placed in the flow stream to remove air bubbles. Data collection began after the temperature of the water blank stabilized at 39.8 °C.

Solution temperature was tightly controlled for all measurements. The procedure described above provided reproducible responses, whereas less rigorous temperature control resulted in poor measurement precision. Solution temperature variations of less than ± 0.1 °C had an adverse effect on measurement reproducibility. This strong temperature dependency is related to the absorptivity of water in this spectral region and the effects of temperature-sensitive hydrogen bonding on the water absorptivity.

Initially, channel signals were monitored after sequential additions of glucose and urea to a buffer blank. In this phase of the experiment, a blank reading was obtained by collection of the four-channel signals for 5 min (15,000 points at 50 Hz) with buffer flowing through the sample cell. After the blank reading, a 75-ml volume of a 3.09-M standard solution of glucose was added to the temperature bath reservoir and hence to the circulating solution. After 5 minutes, a second 75-ml standard addition of glucose was made. Three more 75-ml standard additions were added to the circulating solution with 5-min intervals each time for data acquisition. After the fifth standard addition of glucose, the experiment shifted to urea. In this case, the data-acquisition program was reinitiated, and the first 5 min of this second data-acquisition period corresponded to the glucose solution resulting from the previous five standard additions. A 75-ml volume of a 3.09-M urea standard solution was then added, and the channel responses were recorded for 5 min. Subsequently, second, third, fourth, and fifth 75-ml standard additions were added sequentially with 5 minutes after each addition for data acquisition. This same procedure was followed in a separate experiment, but standard additions of urea were added before the standard additions of glucose. In both cases, the final concentrations of glucose and urea were 309 mM after all standard additions were made.

Data were compiled as an array of $180,000 \times 4$ data points. This data format corresponds to signals from the four detector channels collected over a 60-min period (60 min at 50 Hz gives 180,000 points). Each column in the data array corresponds to a given channel, and each row corresponds to a specific time during the experiment. Signals were originally recorded as raw voltages. We computed relative signals for each channel by dividing raw channel signals by a mean blank signal for that channel and then subtracting one. Composition of the blank solution and period over which the mean is computed must be defined for the relative signals. For the results presented here, the blank solution was buffer, and the mean blank signal was computed over the 5 min (i.e., the first 15,000 time points) of data acquisition. Signal processing was performed with MATLAB (version 5.2, The Math Works, Inc., Natick, Massachusetts), and SigmaPlot (version 4.01, SPSS, Inc., Chicago, Illinois) was used to prepare plots and to perform the regression analysis.

4. Experimental Results

As described previously,¹⁻⁴ the chemical selectivity of a Kromoscopic measurement is governed by the bandpass functions of the individual detector channels. Two requirements are necessary to resolve chemical species within a sample matrix. First, the chemical species to be resolved must possess unique and measurable absorption bands within the overall spectral bandpass of the measurement. Second, the bandpass functions of the individual detector chan-

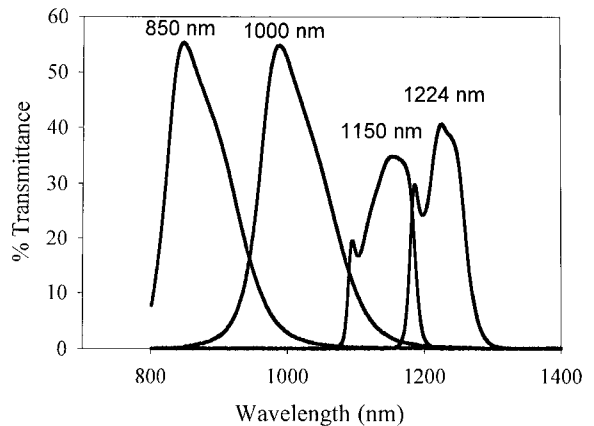


Fig. 2. Transmission spectra of the filters used in the four-channel detector module.

nels must be selected as a group to differentiate these absorption features.

A. Filter Response Functions

At the current stage of development, there is no theory for selecting filter bandpass functions on the basis of the absorption properties of the solute molecules. The ability to preselect filters is further confounded by a lack of reliable absorbance spectral information for glucose and urea throughout the sw-NIR spectral range. Indeed, the absorption characteristics of glucose and urea are so weak and overlapping with respect to water that high-quality absorbance spectra are essentially impossible to obtain experimentally. Glucose and urea spectra over the sw-NIR spectrum are generally dominated by spectral variations associated with the displacement of water, thereby complicating the identification of solute-specific absorption bands. The experimental uncertainties associated with the location, width, and size of absorption bands for glucose and urea preclude the *a priori* selection of filter response functions. For this reason, the filters used in this initial research were selected to span the entire spectral region, thereby ensuring the inclusion of the available glucose and urea information.

The transmission spectra in Fig. 2 correspond to the individual channel filters used in this experiment. These filters are centered at 850, 1000, 1150, and 1224 nm. The superposition of these spectra illustrates the degree of overlap between detector channels. The wavelength of maximum transmittance and spectral bandwidth were selected to span the full wavelength range from 800 to 1300 nm evenly. In this manner, these filters should capture information corresponding to the overtone and the combination vibrational absorption bands within this spectral region for glucose and urea.¹⁷⁻²¹

B. Channel Signals

Analysis of signal-time profiles reveals important differences in the individual channel responses for glucose and urea. The relative channel signals are

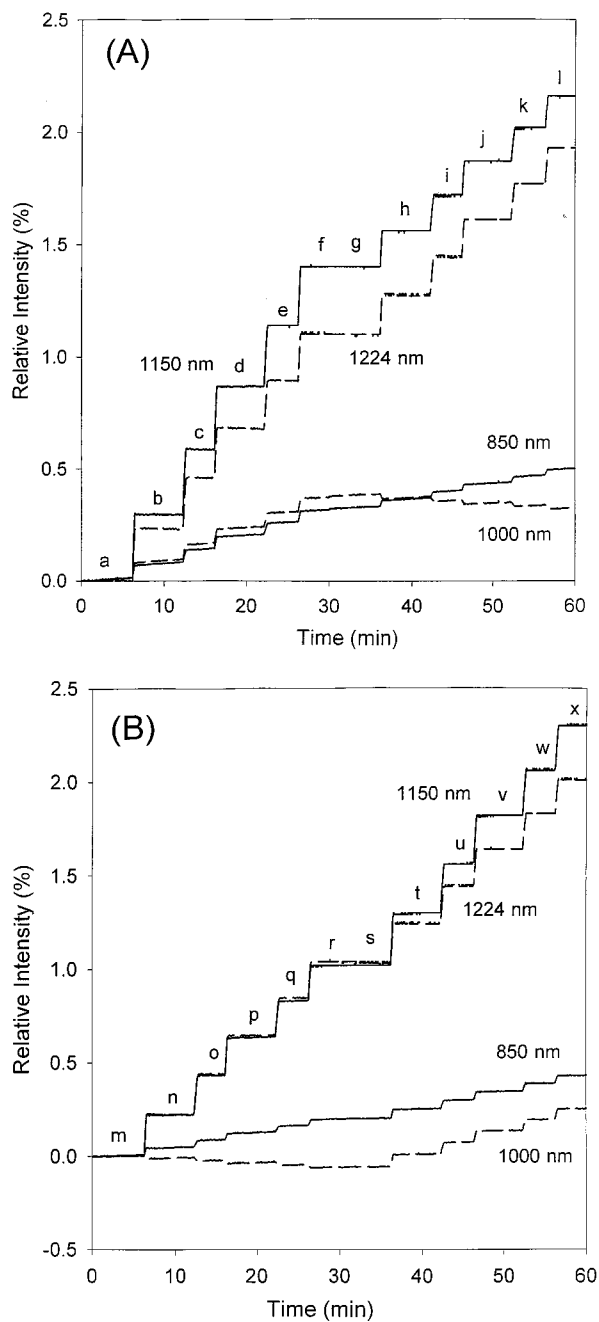


Fig. 3. Four-channel intensity-time traces for experiments in which (A) glucose is added first, followed by urea and (B) urea is added first, followed by glucose. Responses are shown as solid lines for the 850- and the 1150-nm channels and as broken lines for the 1000- and the 1224-nm channels. Letters indicate different glucose-urea solution compositions as explained in Section 3. Solutions correspond to blank buffer (a and m), solutions following a standard addition of glucose (b–f and t–x), and solutions following a standard addition of urea (h–l and n–r). Solutions g and s correspond to points after all the initial solute additions (glucose and urea, respectively) and before additions of the second solute (urea and glucose, respectively).

presented in Fig. 3 for experiments in which the order of addition is glucose followed by urea [Fig. 3(A)] and then urea followed by glucose [Fig. 3(B)]. In these

plots, the relative signal is plotted as a function of time for each individual channel.

The most noticeable aspect of the channel responses shown in Fig. 3 is that the transmitted light intensity increases for nearly all channels as the solute concentration (glucose or urea) increases with each standard addition. These increases in transmittance can be explained by less water in the optical path. Water possesses several well-known absorption bands in this region of the NIR spectrum.^{22–26} As glucose or urea is added, a specific volume of water is displaced, thereby reducing the amount of water in the optical path. The amount of water displacement is different for glucose and urea. The specific molar water displacement is 6.24 for glucose²⁷ and 2.42 for urea,²⁸ which indicates that 6.24 and 2.42 mol of water are displaced for each mole of glucose and urea, respectively. The effect of adding either solute to the circulating buffer solution is to replace a fraction of the solvent molecules with solute. The resulting measured transmittance is a function of the increase in radiant transmission associated with fewer absorbing water molecules and a decrease in transmission caused by absorption from the added solute. Clearly, the results in Fig. 3 indicate that water is the principal absorber at these wavelengths and that displacement of water is the primary factor in the measurement.

Careful analysis of the data reveals that more than simple water displacement is involved. Significant differences in pattern of response are evident for glucose and urea by comparison of the relative signal changes in Figs. 3(A) and 3(B), especially over the first 30 min in each case. The first 30 min in Fig. 3(A) correspond to sequential additions of glucose. The greatest change in transmitted radiant power is observed in the 1150-nm channel with standard additions of glucose. Overall for glucose, the degree of change in transmitted power follows the order 1150-, 1224-, 1000-, and 850-nm channels. In contrast, for urea the order is 1224, 1150, 850, and 1000 nm. Unlike the responses to glucose, changes for the 1224 and 1150-nm channels are approximately equal for urea, with the 1224-nm channel displaying slightly larger changes in signal. The magnitude of the urea response in the 850-nm channel drops considerably relative to the 1224- and 1150-nm channels. The intensity response from the 1000-nm channel actually decreases with increasing urea levels, which might correspond to the urea absorption band reported by Reeves¹⁸ at 1015 nm. This attenuation of the transmitted radiant power by urea is evident in both Figs. 3(A) and 3(B).

The data in Fig. 3 indicate that the primary effect of adding glucose or urea to water is an increase in transmittance because of water displacement. Differences in the specific volume of glucose and urea should result in different amounts of water displaced per mole of solute. For this reason, differences in the absolute magnitude of each channel would be expected for glucose and urea. No differences would be expected, however, between the relative magni-

tudes of the four-channel responses if water displacement were the sole effect. If water displacement were the only effect, then the displacement of the same amount of water by either glucose or urea should result in the same pattern of responses from the four detector channels. Our analysis of Fig. 3 indicates that more than water displacement is involved as glucose and urea elicit a different pattern of channel responses. These observations demonstrate that unique chemical information is embedded within the composite four-channel responses.

C. Vector Profiles

Three-dimensional vector plots can be used to highlight the differences in channel responses for glucose and urea. Such a plot is provided in Figs. 4(A) and 4(B). The axes in these plots correspond to the relative signals measured for three of the four channels. In this presentation of the data, information from one of the four channels is lost. In Figs. 4(A) and 4(B), the axes correspond to the 1000-, 1150-, and 1224-nm channels, and the information associated with the 850-nm channel is lost.

In Fig. 4(A), the raw intensities presented in Figs. 3(A) and 3(B) are plotted in this three-dimensional space. In addition, the mean intensity for each glucose-urea solution is plotted as a single point and labeled with the same identification letter provided in Fig. 3. The a-l data correspond to the experiment in which glucose is added first followed by urea, and the m-x data correspond to the analogous experiment with urea added first followed by glucose. For clarity, these data are presented again in Fig. 4(B). In Fig. 4(B), only the mean intensities are plotted for each solution, the identifying solution letters are removed, the plot is presented at a slightly different angle, and drop lines are provided to better show the response in the x - y plane.

As with the a-l data, five separate data points are evident for the five standard additions of glucose (b-f). In the absence of the superimposed circular points, the raw solution points appear as thick, horizontal lines in this coordinate system. The mean intensity points for glucose follow a linear path with a specific directionality. Lines connecting these points basically follow the same direction and correspond to increasing glucose concentrations as the system equilibrates after each standard addition. By switching from glucose to urea (points g-l), the directionality of the composite response changes rather drastically. Again, the mean intensity points for each urea level follow a linear path in this three-dimensional space. As with glucose, the lines connecting the urea points follow the same direction as the urea vector defined by the points themselves.

Similar response vectors are evident, as shown by the m-x data in Fig. 4(A). Here, the initial points correspond to standard additions of urea (points m-r), which are followed by additions of glucose (points s-x). The corresponding urea and glucose vectors are similar to those presented in the a-l data. The directionality of the glucose and urea vectors are

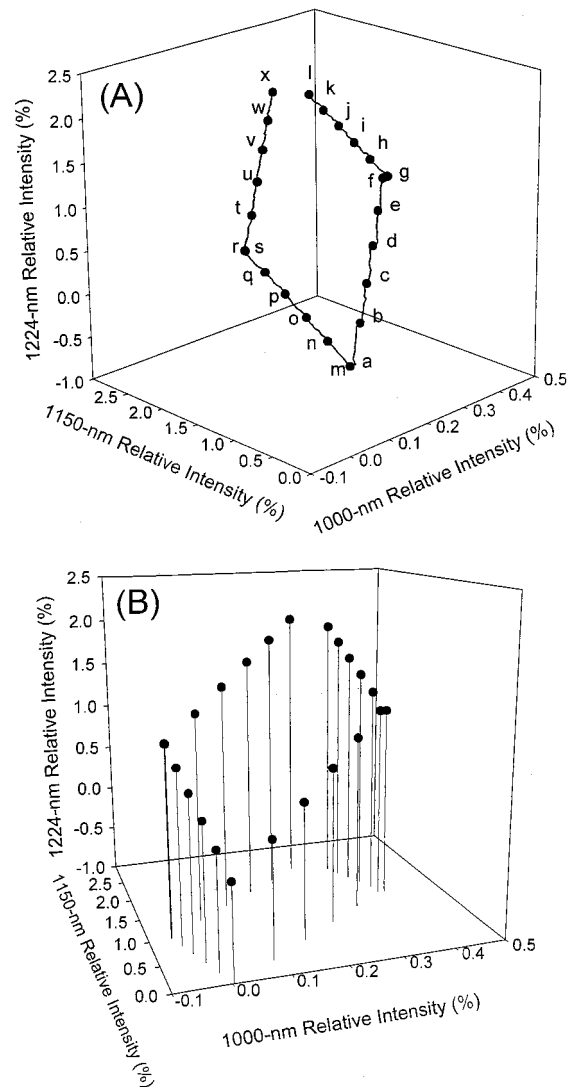


Fig. 4. Three-dimensional vector plots for experiments in which (A) glucose is added first, followed by urea [points a-l in (A)] and urea is added first, followed by glucose [points m-x in (A)]. Axes correspond to relative intensity signals measured from the 1000-, 1150-, and 1224-nm channels. Points correspond to mean intensity values for each solution (a-x) as defined in Section 3 and the Fig. 3 legend. Plot in (B) shows the same data drop lines into the 1000-1150-nm plane.

conserved, which indicates that the direction of the response to glucose is unaffected by urea and that the direction of the urea vector is not altered by glucose. The conservation in directionality is particularly evident, as shown by the drop lines provided in Fig. 4(B) for the 1000-1150-nm plane. Ideally, the two paths (a-l and m-x) should meet at a common point because the same concentrations of glucose and urea exist in the final solutions of both routes. The extent to which these vectors are not perfectly aligned represents between-run variance in the experiment.

A four-dimensional analysis can be performed by computation of the composite responses in the four-dimensional space defined by each detector channel. The directionality of these vectors can be assessed by

measurement of the angle between the glucose and the urea vectors in this four-dimensional space. The angle between the glucose and the urea vectors is 162.6° for the glucose-urea order of addition [points a–f and g–l in Figs. 3(A) and 4(A)]. The angle between these vectors in the urea-glucose order of addition [points m–r and s–x in Figs. 3(A) and 4(A)] is 164.5° . The similarity between these angles demonstrates that the directionality of each vector is conserved in the presence of the other solute.

5. Conclusions

Sensitivity and directionality characterize the Kromoscopic vectors presented in Figs. 4(A) and 4(B) for glucose and urea. Sensitivity of the glucose vector is slightly greater than that for urea. A key feature, however, is the difference in direction of these two vectors. No difference in directionality would be expected for a simple water-displacement effect. Although glucose and urea have different specific molar volumes, and therefore should displace different amounts of water on a per mole basis, no change in the directionality of the vector response should be observed. Removal of water from the optical path should elicit a particular response from each channel, and such responses should remain the same, regardless of solute. The difference in directionality illustrated in Figs. 4(A) and 4(B) clearly indicates that more than simple water displacement is involved. We postulate that differences in the molecular structure of glucose and urea are principally responsible. These findings corroborate those reported earlier by Misner and Block.⁴

The difference in directionality of the analyte vectors is the principal basis for distinguishing glucose and urea. The next issue to be addressed concerns the extent to which such differences can be used to quantify these components independently in binary mixtures. The selection of filters and the dependency of system performance on filter selection are two other critical issues for future investigations.

This research was sponsored by a grant from Selfcare, Inc. The instrumentation was supplied and installed by Optix, LP and their assistance is acknowledged. Finally, Michael Misner's assistance with both hardware and software is greatly appreciated.

References

1. L. A. Sodickson and M. J. Block, "Kromoscopic analysis: a possible alternative to spectroscopic analysis for noninvasive measurement of analytes in vivo," *Clin. Chem.* **40**, 1838–1844 (1994).
2. M. J. Block, "Kromoscopic analysis challenges spectroscopy," *Photonics Spectra* **28**, 135–139 (1994).
3. L. A. Sodickson, "Improvements in multivariate analysis via Kromoscopic measurements," *Spectroscopy* **12**, 13–16, 18, 22, 24 (1997).
4. M. W. Misner and M. J. Block, "The raw data of Kromoscopic analysis," *Spectroscopy* **12**, 20–21 (1997).
5. M. J. Block, "Noninvasive testing," U.S. patent 5,321,265 (14 June 1994).
6. M. J. Block and L. Sodickson, "Noninvasive non-spectrophotometric infrared measurement of blood analyte concentrations," U.S. patent 5,424,545 (13 June 1995).
7. M. J. Block and L. Sodickson, "Non-spectrophotometric measurement of analyte concentrations and optical properties of objects," U.S. patent 5,434,412 (18 July 1995).
8. M. J. Block and L. Sodickson, "Methods of minimizing scattering and improving tissue sampling in noninvasive testing and imaging," U.S. patent 5,672,875 (30 September 1997).
9. L. Sodickson and M. J. Block, "Nonspectrophotometric measurement of analyte concentrations and optical properties of objects," U.S. patent 5,818,044 (6 October 1998).
10. L. Sodickson, H. E. Guthermann, and M. J. Block, "Rapid noninvasive optical analysis using broad bandpass spectral processing," U.S. patent 5,818,048 (6 October 1998).
11. M. J. Block, "Noninvasive IR transmission measurement of analyte in the tympanic membrane," U.S. patent 6,002,953 (14 December 1999).
12. L. Sodickson, H. E. Guthermann, and M. J. Block, "Rapid noninvasive optical analysis using broad bandpass spectral processing," U.S. Patent 6,028,311 (22 February 2000).
13. M. A. Arnold and G. W. Small, "Determination of physiological levels of glucose in aqueous matrix with digitally filtered Fourier transform near-infrared spectroscopy," *Anal. Chem.* **62**, 1457–1464 (1990).
14. H. Chung, M. A. Arnold, M. Rhiel, and D. W. Murhammer, "Simultaneous measurements of glucose, glutamine, ammonia, lactate, and glutamate in aqueous solutions by near-infrared spectroscopy," *Appl. Spectrosc.* **51**, 270–276 (1996).
15. K. H. Hazen, M. A. Arnold, G. W. Small, "Measurement of glucose in water with first overtone near infrared spectra," *Appl. Spectrosc.* **52**, 1597–1605 (1998).
16. R. J. McNichols and G. L. Coté, "Optical glucose sensing in biological fluids: an overview," *J. Biomed. Opt.* **5**, 5–16 (2000).
17. O. H. Wheeler, "Near infrared spectra of organic compounds," *Chem. Rev.* **59**, 629–666 (1959).
18. J. B. Reeves II, "Effects of water on the spectra of model compounds in the short-wavelength near infrared spectral region (14,000–9091 cm^{-1} or 714–1100 nm)," *Near Infrared Spectrosc.* **2**, 199–212 (1994).
19. J. D. Ingle and S. R. Crouch, *Spectrochemical Analysis* (Prentice-Hall, N.J., 1988).
20. O. S. Khalil, "Spectroscopic and clinical aspects of noninvasive glucose measurements," *Clin. Chem.* **45**, 165–177 (1999).
21. M. Kohl, M. Essenpreis, and M. Cope, "The influence of glucose concentration upon the transport of light in tissue-simulating phantoms," *Phys. Med. Biol.* **40**, 1267–1287 (1995).
22. K. Buijs and G. R. Choppin, "Near-infrared studies of the structure of water. I. Pure water," *J. Chem. Phys.* **39**, 2035–2041 (1963).
23. J. G. Bayly, V. B. Kartha, and W. H. Stevens, "The absorption spectra of liquid phase H_2O , HDO , and D_2O from 0.7 μm to 10 μm ," *Infrared Phys.* **3**, 211–223 (1963).
24. J. Lin and C. W. Brown, "Near-IR spectroscopic determination of NaCl in aqueous solution," *Appl. Spectrosc.* **46**, 1809–1815 (1992).
25. J. Lin and C. W. Brown, "Spectroscopic measurement of NaCl and seawater salinity in the near-IR region of 680–1230 nm," *Appl. Spectrosc.* **47**, 239–241 (1993).
26. J. Lin and C. W. Brown, "Universal approach for determination of physical and chemical properties of water by near-IR spectroscopy," *Appl. Spectrosc.* **47**, 1720–1727 (1993).
27. R. C. Weast, ed., "Concentration properties of aqueous solutions: conversion tables," in *Handbook of Chemistry and Physics*, 56th ed. (CRC Press, Cleveland, Ohio, 1975), p. D-230.
28. Ref. 27, p. D-265.